Citation: Molecular Therapy — Methods & Clinical Development (2016) **3,** 16010; doi:10.1038/mtm.2016.10
Official journal of the American Society of Gene & Cell Therapy

www.nature.com/mtm

ARTICLE

Comparative study of human embryonic stem cells (hESC) and human induced pluripotent stem cells (hiPSC) as a treatment for retinal dystrophies

Marina Riera[1,2], Laura Fontrodona[1], Silvia Albert[3,4], Diana Mora Ramirez[1,5], Anna Seriola[3], Anna Salas[1], Yolanda Muñoz[3], David Ramos[6,7], Maria Paz Villegas-Perez[8], Miguel Angel Zapata[1], Angel Raya[3,9,10], Jesus Ruberte[6,7,11], Anna Veiga[3] and Jose Garcia-Arumi[1,2]

Retinal dystrophies (RD) are major causes of familial blindness and are characterized by progressive dysfunction of photoreceptor and/or retinal pigment epithelium (RPE) cells. In this study, we aimed to evaluate and compare the therapeutic effects of two pluripotent stem cell (PSC)-based therapies. We differentiated RPE from human embryonic stem cells (hESCs) or human-induced pluripotent stem cells (hiPSCs) and transplanted them into the subretinal space of the Royal College of Surgeons (RCS) rat. Once differentiated, cells from either source of PSC resembled mature RPE in their morphology and gene expression profile. Following transplantation, both hESC- and hiPSC-derived cells maintained the expression of specific RPE markers, lost their proliferative capacity, established tight junctions, and were able to perform phagocytosis of photoreceptor outer segments. Remarkably, grafted areas showed increased numbers of photoreceptor nuclei and outer segment disk membranes. Regardless of the cell source, human transplants protected retina from cell apoptosis, glial stress and accumulation of autofluorescence, and responded better to light stimuli. Altogether, our results show that hESC- and hiPSC-derived cells survived, migrated, integrated, and functioned as RPE in the RCS rat retina, providing preclinical evidence that either PSC source could be of potential benefit for treating RD.

Molecular Therapy — Methods & Clinical Development (2016) **3**, 16010; doi:10.1038/mtm.2016.10; published online 16 March 2016

INTRODUCTION

The retinal pigment epithelium (RPE) is a polarized monolayer of epithelial cells that rests on Bruch's membrane, between the choriocapillaries and the neural retina. RPE cells create the external blood–retina barrier and have multiple roles in maintaining photoreceptor health and visual function: they are involved in retinol recycling, absorption of stray light, nutrient transport, phagocytosis of photoreceptor outer segments (OS), and trophic factor secretion.[1,2] RPE dysfunction, which usually leads to the damage and death of photoreceptor cells, occurs in several retinal dystrophies (RD), such as retinitis pigmentosa (RP), which is the most frequent inherited RD with a prevalence of 1:4,000 and more than 1 million people affected worldwide.[3,4] To date, more than 60 different genes and over 3,000 different disease alleles have been associated with classical forms of RP. Whether this great genetic heterogeneity ultimately converges on one or several retinal cell death pathways is poorly understood, and this lack of knowledge has hindered the efforts to elucidate efficient therapeutic strategies.[5]

Some of the current therapeutic approaches for RD use gene delivery systems, treatment with neurotrophic growth factors, antiapoptotic agents, ribozyme therapy, RNA interference, dietary supplementation, or cell replacement.[6] However, most of these treatments are only effective in preventing or slowing down the progression of the dystrophy, and are less efficient when used to treat advanced stages of the disease.[7] Within this context, cell therapies are able to reverse degeneration and vision loss to a greater extent than any other treatment available.[5] In fact, over the past decade, studies with pluripotent stem cells (PSCs) for disease modelling and treatment of incurable diseases have gained momentum in the field of regenerative medicine.[8] The ability of PSCs to provide an unlimited supply of viable and specialized cell types, together with the advantages of the retina for this kind of

The last two authors share senior authorship

[1]Ophthalmology Research, Vall d'Hebron Research Institute (VHIR), Barcelona, Spain; [2]Institut de Microcirurgia Ocular (IMO), Barcelona, Spain; [3]Center of Regenerative Medicine in Barcelona (CMRB), Barcelona, Spain; [4]Department of Human Genetics, Radboud University Medical Center, Nijmegen, The Netherlands; [5]Department of Surgery, Faculty of Medicine, Universitat Autònoma de Barcelona Bellaterra, Spain; [6]Center of Animal Biotechnology and Gene Therapy (CBATEG), Universitat Autònoma de Barcelona, Bellaterra, Spain; [7]CIISA, Faculdade de Medicina Veterinaria, Universidade de Lisboa, Lisboa, Portugal; [8]Ophthalmology Department, Faculty of Medicine, Universidad de Murcia, Murcia, Spain; [9]Institució Catalana de Recerca i Estudis Avançats (ICREA), Barcelona, Spain; [10]Center for Networked Biomedical Research on Bioengineering, Biomaterials and Nanomedicine (CIBER-BBN), Madrid, Spain; [11]Department of Anatomy and Animal Health, School of Veterinary Medicine, Universitat Autònoma de Barcelona, Bellaterra, Spain.
Correspondence: M Riera and S Albert (genetica.riera@imo.es; silvia.albert@radboudumc.nl)
Received 19 January 2016; accepted 27 January 2016

therapy (*i.e.*, the eye is easily accessible, the clear media permits direct visualization following intervention, and the immune privilege conferred by blood-retina barrier), make of cell therapy one of the most promising treatments for RD.[9] At present, all major retinal cell types, RPE cells among them, can be differentiated from both human embryonic stem cells (hESCs) and human-induced pluripotent stem cells (hiPSCs).[10–14] The success in the use of such cells as biological therapy will depend on the ability of grafted cells to survive after transplantation, migrate toward the desired location and differentiate into functional target cells.[15]

The Royal College of Surgeons (RCS) rat is a good model for exploring potential treatment approaches for RD.[16,17] These animals harbor a mutation in the gene that encodes MERTK, a transmembrane tyrosine kinase expressed in RPE cells that plays a crucial role in the signal transduction pathway involved in the phagocytosis of photoreceptor OS.[18] In this animal model, apoptosis of photoreceptors arises from the third week of age and progressively affects the majority of cells, producing a severely impaired retinal function at 2–3 months.[19] Several cell types have been tested for RPE cell replacement in this model, including RPE and non-RPE immortalized cell lines,[16,20–27] RPE derived from hESCs,[12,28] and RPE derived from hiPSCs.[29,30] When the intervention was performed at early stages of the disease, these studies achieved successful morphological and functional rescue. However, further studies are needed to elucidate whether cell therapy may be effective if introduced at later stages of degeneration. This is clinically important, as cell-based therapies are more likely to be applied at a time when the vision in most patients is already compromised. Moreover, a comprehensive study comparing the use of the two types of PSCs is still lacking. Within this context, we aimed at: (i) developing a well-defined culture protocol to direct the differentiation of hESC and hiPSC lines into RPE cells, (ii) transplanting them into the subretinal space of RCS rats at postnatal day 21 or 42 (P21 or P42), (iii) assessing their migration, integration, survival and functionality, and (iv) determining any differences between the two PSC types.

RESULTS

Differentiation and expansion of human ES and iPS cell lines into mature RPE

Both hESC and hiPSC lines were successfully differentiated into RPE-like cells using a 12-week protocol in which PSCs, cultured on Matrigel-coated dishes, were kept in RPE-specific medium until the end of the experiment (see Supplementary Materials and Methods and Supplementary Figure S1a). Pigmented cells that appeared in the culture after 5 weeks were purified by hand picking at week 6, and homogeneous cultures consisting on pigmented epithelial monolayer cobblestone-shaped cells could be obtained and expanded from either PSC source (see Supplementary Figure S1b).

Transmission electron microscopy revealed the typical morphology and structural characteristics of RPE, including the presence of melanosome granules, polarized monolayer cell distribution with apical microvilli and tight junctions between cells (Figure 1a). Comparable results were obtained with both cell lines and were reproducible in different experiments (data not shown).

Expression profile of differentiated cells

Homogeneous RPE cell cultures were positive for the expression of several neural retina markers such as PAX6, OTX2, and CHX10; and for the RPE-specific markers BEST1, MITF, RPE65, and the tight junction marker ZO-1 (Figure 1b).

Quantitative real-time PCR analyses of RPE differentiated from hESCs and hiPSCs showed a progressive decrease in the expression of the pluripotency marker *OCT3/4*, and increased expression of genes essential for eye development, such as the neural markers *PAX6* and *RX*, the visual cycle gene *CRALBP*, the genes encoding the transcription factors *MITF* and *OTX2*, the pigment synthesis-related gene *SILVER* (*SIL*), the phagocytic marker *MERTK*, and the gene encoding the pigment epithelium-derived factor and neurotrophic factor (*PEDF*) (Figure 1c). Except for *OTX2*, the expression of which was approximately threefold higher in hiPSC-derived RPE cells compared with those differentiated from hESC, the expression level of genes related with retina/RPE development was similar in RPE cells derived from either PSC source.

Human PSC-derived RPE cells survive in the rat subretinal space and integrate within the host RPE

RCS rats were injected subretinally with RPE cells differentiated from hESC or hiPSC (RPE-injected eyes), or with differentiation medium alone (sham-injected eyes) (see Supplementary Video S1 and Table 1). To avoid the introduction of transgenic markers such as GFP, which could increase the risk of altering gene expression or cellular functions, human cells were transiently stained with a green fluorescent dye (CellTracker), which allowed tracking the cell grafts *in vivo* for the first 5–6 days after transplantation (Figure 2a).

At 5 weeks postinjection (PI), human cells were found integrated into the rat retina as scattered single-cell units, occupying the subretinal space as extensive laminar sheets, or in discrete rosette-like formations (Figure 2b). Grafted cells were never observed within the cellular layers of the neurosensory retina.

To study the distribution and integration of human transplants further, we isolated the posterior pole of transplanted eyes and removed the retina to expose whole RPE monolayers. In all RPE-injected eyes (5 weeks PI, $n = 4$; 8 weeks PI, $n = 6$ and 12 weeks PI, $n = 8$), human RPE grafts covered an area comparable with the original bleb observed by color fundus imaging on the day of injection (see Supplementary Figure S2). We also found that human cells formed tight junctions between each other and established associations with the host tissue in all cases examined up to 12 weeks PI (Figure 2c). Comparable distribution and integration patterns were observed in transplants of RPE cells differentiated either from hESCs or hiPSCs.

Expression of RPE-specific markers and phagocytosis of host OS by transplanted cells

After observing that grafts derived from both hESCs and hiPSCs properly integrated into rat retinas, we determined if such RPE transplants continued to express RPE markers such as CRALBP, which was expressed by the same cells before transplantation at the end of the *in vitro* differentiation process (Figure 1c). We found that hESC- and hiPSC-derived RPE cells were able to maintain CRALBP expression for at least 5 weeks PI. Moreover, most RPE cells were nonproliferative as shown by immunostaining of Ki67 (Figure 3a).

To determine the phagocytic ability of the transplanted cells *in vivo*, a human-specific marker antibody cocktail (HSM) was used together with an antirhodopsin antibody. We were able to demonstrate endocytosis of rhodopsin-positive debris by both human RPE cell types (Figure 3a). To confirm that human RPE cells were functional in the host retina, we monitored autofluorescence (AF) as a biomarker of phagocytosis and visual cycling. We observed a

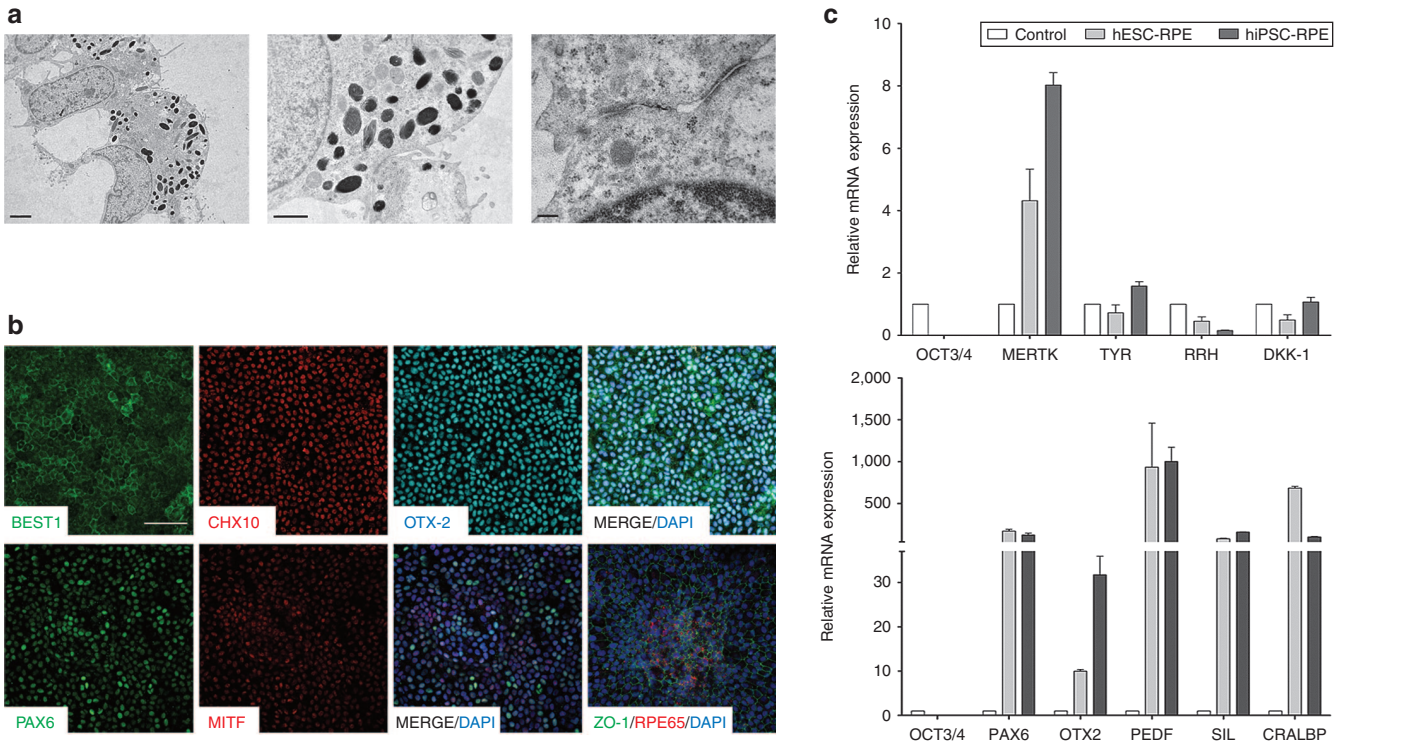

Figure 1 Characterization of differentiated RPE cells. (**a**) Electron micrograph showing basal nuclei and apical microvilli (left panel), melanin granules (central panel) and tight junction establishment (right panel) at 12 weeks of differentiation. (**b**) Immunocytochemical analysis of differentiated cells confirming protein expression of genes responsible for neural retina and RPE development (PAX6, MITF, CHX10 and OTX2) and markers of mature RPE (BEST1, RPE65 and ZO-1). Pluripotency marker OCT4 started decreasing after 4 days of differentiation. Positive PAX6 and MITF cells were negative for OCT4 marker (data not shown). (**c**) Gene expression profile by real-time PCR of differentiated RPE cells. Undifferentiated hPSC cell sample was used as the zero set point (control). Images shown in **a** and **b** sections were obtained in hiPSC differentiated cells, but comparable results were observed in hESC-derived cells. **a** Bars = 2 µm (left panel); 1 µm (middle panel); 0.2 µm (right panel). **b** Bar = 50 µm. Data are presented as mean ± SEM. RPE, retinal pigment epithelium.

Table 1 Groups of transplanted animals

		Injected material		
Day of injection	*Euthanasia (weeks PI)*	*hESC-RPE*	*hiPSC-RPE*	*Medium*
P21	5	11	12	14
	8	12	15	4
	12	12	12	4
P42	5	4	4	4
Total (*n*)		39	43	26

The number of eyes (*n*), the type of injected material (hESC- or hiPSC-RPE, or medium), the postnatal day of injection (P21 or P42), and the week of euthanasia (5, 8 or 12 weeks PI) are shown for each group.

clear difference in the distribution pattern of AF between grafted, nongrafted regions, and sham-injected eyes. Grafted areas of RPE-injected eyes (either from hESC- or hiPSC-derived cells) presented lower levels of AF, showing a punctate pattern localized near the RPE layer, whereas nongrafted areas of the same RPE-injected eyes or sham-injected eyes showed high AF levels, with a thick and diffuse pattern filling the whole subretinal space (Figure 3b).

We next analyzed the ultrastructure of the grafted areas in RPE-injected eyes at 12 weeks PI. Sham-injected eyes presented a loss of photoreceptor nuclei and a thickening of the debris layer, consisting of membranous waste material originating from the unphagocytosed rod OS (Figure 4a). We observed alterations in the ultrastructure of the retina of RCS sham-injected eyes in comparison with Long–Evans wild-type eyes. Specifically, the number of basal infoldings was diminished and many vacuolar-like spaces containing membrane-bound degenerated organelles were observed (Figure 4b and Supplementary Figure S3). No ultrastructural alterations of Bruch's membrane were observed in any of the eyes studied (Figure 4c). In grafted areas of RPE-injected eyes, the number of RPE basal infoldings and morphology were recovered in the area close to the transplanted cells (Figure 4b–d), and many round phagosomes packed with OS disk membranes were evident in these regions (Figure 4d), but not in sham-injected eyes. At the same time, an amelioration of organization in several OS was observed in RPE-injected eyes (see Supplementary Figure S3).

Protection of rat photoreceptors against gliosis and apoptosis by RPE cell replacement

By immunostaining retinas at 5 weeks PI, we studied expression levels and distribution of GFAP, an indicator of retinal stress, and found decreased levels in the grafted areas compared with nongrafted areas of the same eyes and with sham-injected eyes (Figure 5a). Moreover, in grafted areas the expression of this protein was restricted to the optic nerve fiber, the ganglion cells, and the inner plexiform layers, whereas in nongrafted areas and sham-injected eyes GFAP was also detected in the inner and outer nuclear layers (INL and ONL), showing a more severe gliosis phenomenon

in regions and eyes that did not receive the cell treatment. Likewise, we explored the capacity of human transplants to delay the activation of photoreceptor-programmed cell death in RCS rats. By performing TUNEL (terminal deoxynucleotidyl transferase-dUTP nick end labelling) analyses on retina cryosections, we noted a strong and consistent reduction in the number of apoptotic photoreceptor cells when comparing grafted versus nongrafted areas and sham-injected eyes (Figure 5b). Similar results were obtained in hESC- and hiPSC-grafted areas, as both gliosis and apoptosis parameters were reduced in all cases.

Therapeutic effect of human transplanted cells during retinal degeneration

At 5 weeks PI of P21 injected rats, retinal layers were better conserved in grafted areas. This preservation extended beyond the transplanted region covered by the graft (Figure 6a,b). In particular, grafted areas displayed inner and outer segments (IS + OS) that were longer than the comparable measurements in nongrafted areas or in sham-injected eyes in all conditions. Despite the progression of the disease, grafted areas of RPE-injected eyes showed the same degree of preservation (around 30–40%) at 5, 8, and 12 weeks after injection (Figure 6c).

Consistent with these observations, we also found that the number of ONL cell rows was preserved up to 12 weeks PI, showing 70% of preservation in the injected regions at all stages. In particular, at 5 weeks PI ~10 cell rows were preserved in grafted areas, compared with only 3 rows detected in nongrafted areas or in sham-injected eyes. The protection against degeneration was maintained until 8 weeks PI, since the number of ONL cell rows was almost the same as at 5 weeks PI. Nevertheless, the decrease in the number of rows with age was evident at 12 weeks PI, when it diminished from 10 to 5–6. Despite this, the number of nuclei rows was still higher in grafted areas than in nongrafted areas or sham-injected eyes, where a discontinuous single layer of nuclei could be observed (Figure 6c). No significant differences were observed when comparing IS + OS thickness or ONL cell rows between hESC- or hiPSC-injected eyes.

Interestingly, in grafted areas of P21 RPE-injected rats, we could accurately delineate the three nuclear layers (ONL, INL, and GCL) and the two plexiform layers (IPL and OPL) for up to 12 weeks, in contrast with the overlapping INL and ONL observed in nongrafted areas and in sham-injected eyes from 8 weeks PI (see Supplementary Figure S4a,b).

In an attempt to outline the benefits of these cell therapies when applied to an advanced degenerated eye, we also transplanted animals at 42 days of age (P42) and their eyes were histologically analyzed at 5 weeks PI. Here, no differences were observed in terms of IS + OS thickness between groups, while the number of ONL cell rows did show a certain level of preservation in grafted areas of both hESC- and hiPSC-injected eyes (more than four cell rows were maintained in comparison with the single cell row observed in nongrafted areas of the same eyes or in sham-injected eyes) (see Supplementary Figure S5c,d).

No tumor formation was observed in the histological examinations during the entire study.

Preservation of electroretinographic activity in RCS rats after stem cell-based RPE therapy

The preservation of visual function was statistically significant in grafted areas of P21 injected rats when stimulated at 4,000 or 16,000 cd·seconds/m^2 at 5 weeks PI (Figure 7a,b). Indeed, the mean

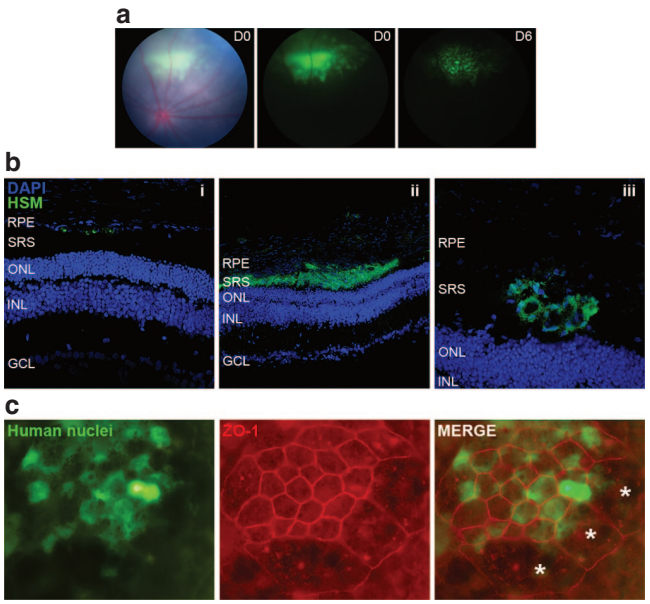

Figure 2 Human cells survive and integrate within the host tissues. (**a**) Fundus images showing the location of the grafted cells within the subretinal space of RCS rat after transplantation at day 0 (middle panel) and after 6 days (right panel). Green fluorescence observed is emitted from Cell Tracker, which was used to label transplanted cells transiently. (**b**) Immunohistochemical analysis was performed to visualize the human cells distribution among rat retina layers at 5 weeks PI of P21 injected rats. Human cells are shown in green, stained with a cocktail of human-specific markers (HSM). Human cells were found in three different locations: (i) adjacent to the host RPE, (ii) in the subretinal space adopting laminar or (iii) rosette-like structures. These images were obtained in hiPSC-injected eyes and are shown as representative examples, but similar results were achieved in hESC-injected eyes. (**c**) A RPE flat mount preparation of a hESC-injected eye after 12 weeks of transplantation shows the establishment of tight junctions (ZO-1) between the human cells themselves and the human and rat cells. Asterisks (*) denote rat cells, which are larger and are not stained by human nuclei marker. RCS, Royal College of Surgeons; RPE, retinal pigment epithelium; SRS, subretinal space; ONL, outer nuclear layer; ONL, outer nuclear layer; INL, inner nuclear layer; GCL, ganglion cell layer.

b-wave amplitude of both hiPSC-RPE- and hESC-RPE-injected regions was similar, but significantly higher than the amplitudes observed in nongrafted areas or in sham-injected eyes (around 40% higher at 4,000 cd·seconds/m^2, and 46% at 16,000 cd seconds/m^2). Although at 8 weeks PI b-wave amplitudes were clearly attenuated, preservation of retinal function was still observed since focal electroretinography (ERG) recordings also showed significant rescue in grafted areas. However, by 12 weeks PI, b-wave amplitudes became nonexistent and no differences were observed between the groups.

In the animals injected at P42, no visual response was detected at 5 weeks PI, neither in grafted areas nor in nongrafted areas or sham-injected eyes (data not shown).

DISCUSSION

We successfully established an efficient and reproducible method of RPE cell production from hESCs and hiPSCs. We were able to isolate and purify RPE cells from both cell lines by selecting pigmented colonies of cobblestone-shaped cells. Both RPE cell lines were characterized and the expression of RPE-specific markers confirmed the cell lineage.

Once differentiated, human cells were transplanted by trans-scleral injection into the subretinal space of the rat retina (see

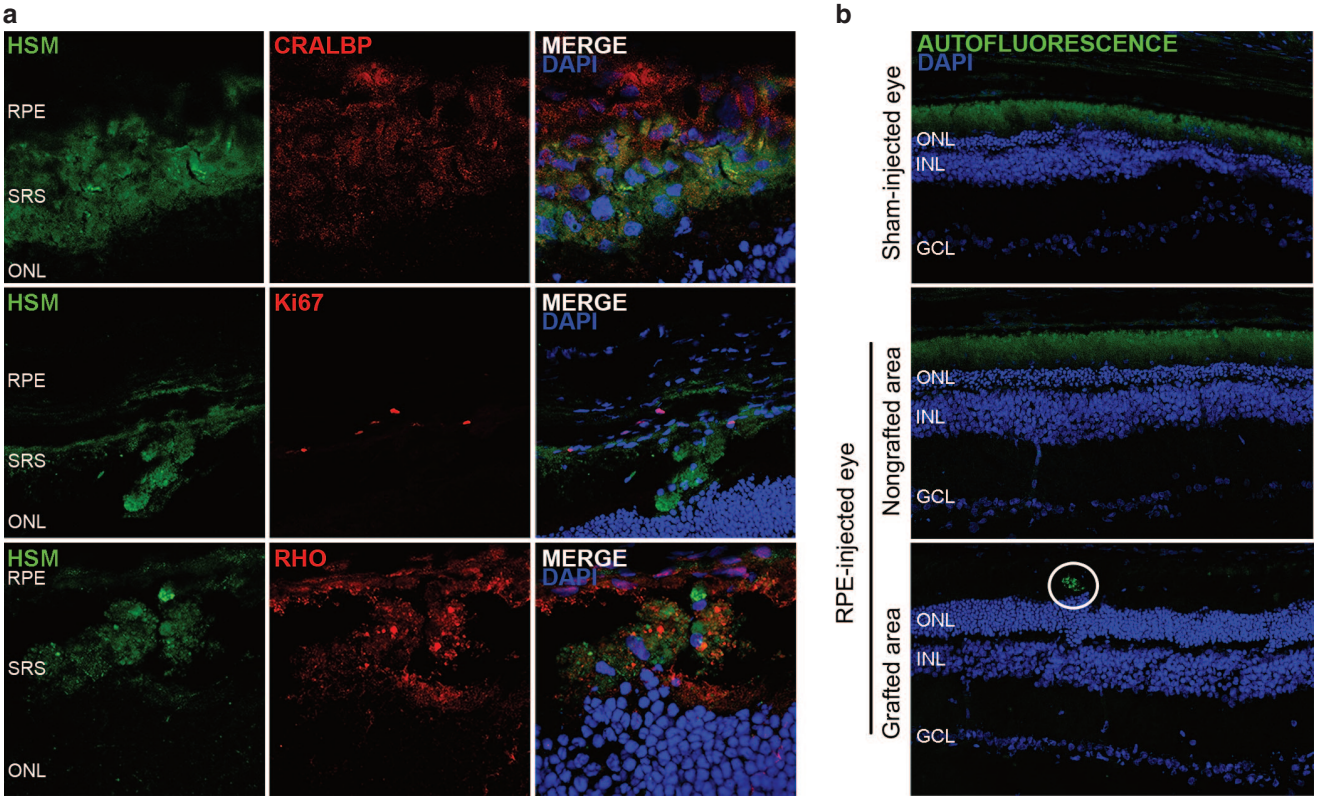

Figure 3 Transplanted cells maintain RPE cell marker expression, phagocytosed rhodopsin material, and decreased autofluorescence levels at 5 weeks PI. (**a**) Grafted cells are positive for CRALBP and mostly negative for Ki67. Rhodopsin-positive material is found within the cell membrane of HSM-labelled cells. (**b**) Autofluorescence in sham-injected eyes and in nongrafted areas was detected scattered all over the SRS, whereas in grafted areas it was limited to discrete spots of the RPE cell layer. Representative images of hiPSC-injected eyes are shown, but similar results were obtained in hESC-injected eyes. RPE, retinal pigment epithelium; SRS, subretinal space; ONL, outer nuclear layer; ONL, outer nuclear layer; INL, inner nuclear layer; GCL, ganglion cell layer.

Supplementary Video S1). At 5 weeks PI, we found human cells in proximity to the host RPE, forming multilayered aggregates in the subretinal space, or integrated as a monolayer. Irrespective of the graft location, ONL was preserved in all cases, indicating that proper integration of human cells in the host RPE would not be a major problem for the treatment to become efficient. Nevertheless, it would be interesting to determine which factors are responsible for graft localization, and whether or not heterogeneous graft location could be controlled to reach a more reliable, accurate, and reproducible method of cell transplantation and integration. Despite the heterogeneity, human cells were always found close to the RPE and, contrary to other studies,[28] they were never found invading cellular layers of the neural retina. This is of high clinical relevance, since the integration of the injected cells into cell layers other than the RPE would alter the structure of such a complex tissue where the proper connections among different cell types are essential to transmit the electrical signal accurately.

Our findings support the view that grafted cells are able to establish tight junctions between each other and with host RPE cells, as shown by ZO-1 staining. These cell–cell adhesions are crucial not only for the maintenance of the blood–retinal barrier, but also for preserving the morphological integrity of the tissue, and for controlling the differentiation and proliferation of epithelial cells.[31] In fact, we have shown that grafted cells are positive for CRALBP (a typical RPE marker) and do not express Ki67 (an indicator of proliferation). Thus, the appropriate formation of these junctions among grafted cells might be imperative to sustain their RPE cell fate and inhibit their proliferation, two key aspects in terms of functionality and safety of the procedure.

One critical role of RPE includes the maintenance of photoreceptor integrity by daily phagocytosis of photoreceptor debris,[1] a function that is impaired in RCS rats owing to the recessive *Mertk* mutation. Here, we showed that grafted cells were able to replace the function that the host RPE lacks and restore phagocytosis of the OS in the RCS rat retina, since rhodopsin granules were found within the human cells and phagosomes were present in RPE cells at the grafted area after 12 weeks of injection. The restoration of RPE phagocytosis had beneficial effects on retinal morphology as we found that photoreceptor OS were better preserved in grafted areas. Moreover, AF levels were clearly decreased in grafted areas, compared with the thick and diffuse AF signal present in nongrafted areas and sham-injected eyes. Notably, we have shown that AF in grafted areas was almost abolished, in contrast with other studies where AF of transplanted regions was not completely reduced, where transplanted cells could be undergoing premature ageing or performing an incomplete ingestion process.[30] If true, the slight AF observed in our study might be due to a better preservation of the photoreceptor/RPE complex.[32]

The presence of human cells in the RCS rat subretinal space was capable of slowing down the progression of the disease. At histological levels, the rate at which the photoreceptor nuclei were lost was lower in grafted than in nongrafted areas and sham-injected eyes. We also found that at 5 and 8 weeks PI programmed cell death was activated in areas that did not receive the cell therapy. Similarly, GFAP

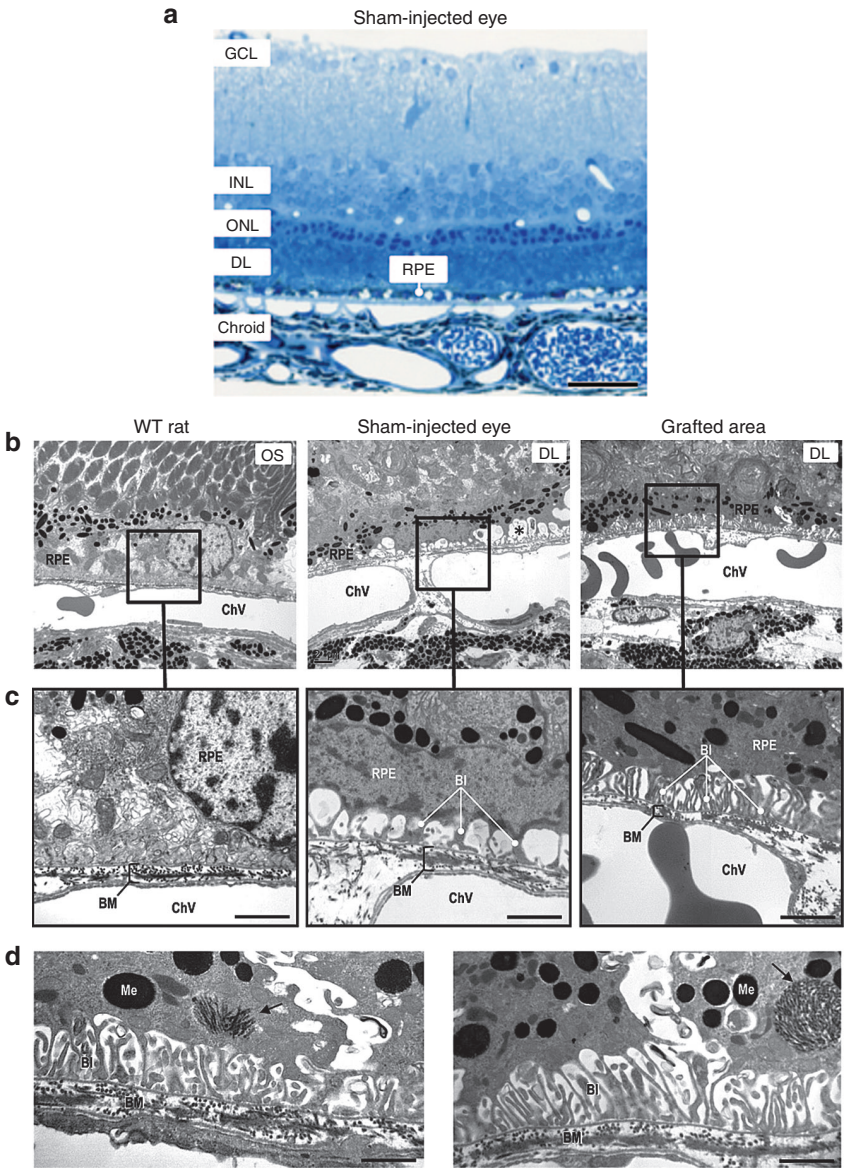

Figure 4 Light and electron microscopy images from WT rats, sham- and RPE-injected RCS rats. (**a**) Semi-thin section stained with methylene blue showing a thickness reduction in the outer nuclear layer and a thick debris layer of unphagocytosed rod outer segments in a RCS sham-injected rat. (**b**, **c**) A reduction of RPE basal infoldings and the presence of vacuole-like spaces (asterisk) can be seen at ultrastructural level in sham-injected RCS rats. This lesion was restored in RPE-injected RCS rats. (**d**) Autophagosomes (arrow) containing outer segment disk membranes were observed in RPE-injected RCS rats. Bars: **a**, 27 µm; **c**, 1.2 µm; **d**, 0.97 µm. BI, basal infoldings; BM, Bruch's membrane; ChV, choroidal vessel; Me, melanosome; GCL, ganglion cell layer; INL, inner nuclear layer; ONL, outer nuclear layer; DL, debris layer; RPE, retinal pigment epithelium; OS, outer segment.

was upregulated in nongrafted areas and in sham-injected eyes. This implies an activation of reactive gliosis in astrocytes and Müller cells, which usually leads to their hypertrophy onto the photoreceptor and vitreal surfaces. Besides, and contrary to grafted areas, prolongations of GFAP-expressing cells reached the outer retina, where GFAP upmodulation has been previously associated with a disruption of the RPE and the blood–retina barrier.[33] Taken together, these results showed how the transplanted cells successfully protected the retina from both apoptosis and glial stress. Nevertheless, despite this clear effect slowing down disease progression, human RPE cells were only able to delay photoreceptor apoptosis for up to 8 weeks. However, at 12 weeks PI, we could still demonstrate a certain degree of ONL preservation in proximity to the grafts. A relationship between the thickness of the ONL and the electroretinographic activity could be established, since at 5 and 8 weeks PI grafted areas with preserved ONL cell row number displayed improved ERG responses compared with nongrafted regions. Nevertheless, as similarly observed in other studies,[12] at 12 weeks PI, the retina did not respond to light stimuli anymore, which suggests that a minimum number of ONL cell rows are necessary to trigger the visual signal cascade. In this sense, it would be interesting to investigate novel methods to better sustain the preservation of photoreceptor cells and maintain photoreceptor survival for longer time periods. For this, several aspects should be considered: first, the number of transplanted cells could be one of the limiting factors; low numbers of cells might not be sufficient to reduce the progression of the disease, but transplantation of a high number of cells in the limited subretinal space could disorganize the multilayered structure of the retina. Second, the use of protocols based on repeated cell injection could be considered, but would not ensure long-term photoreceptor maintenance since our results support that

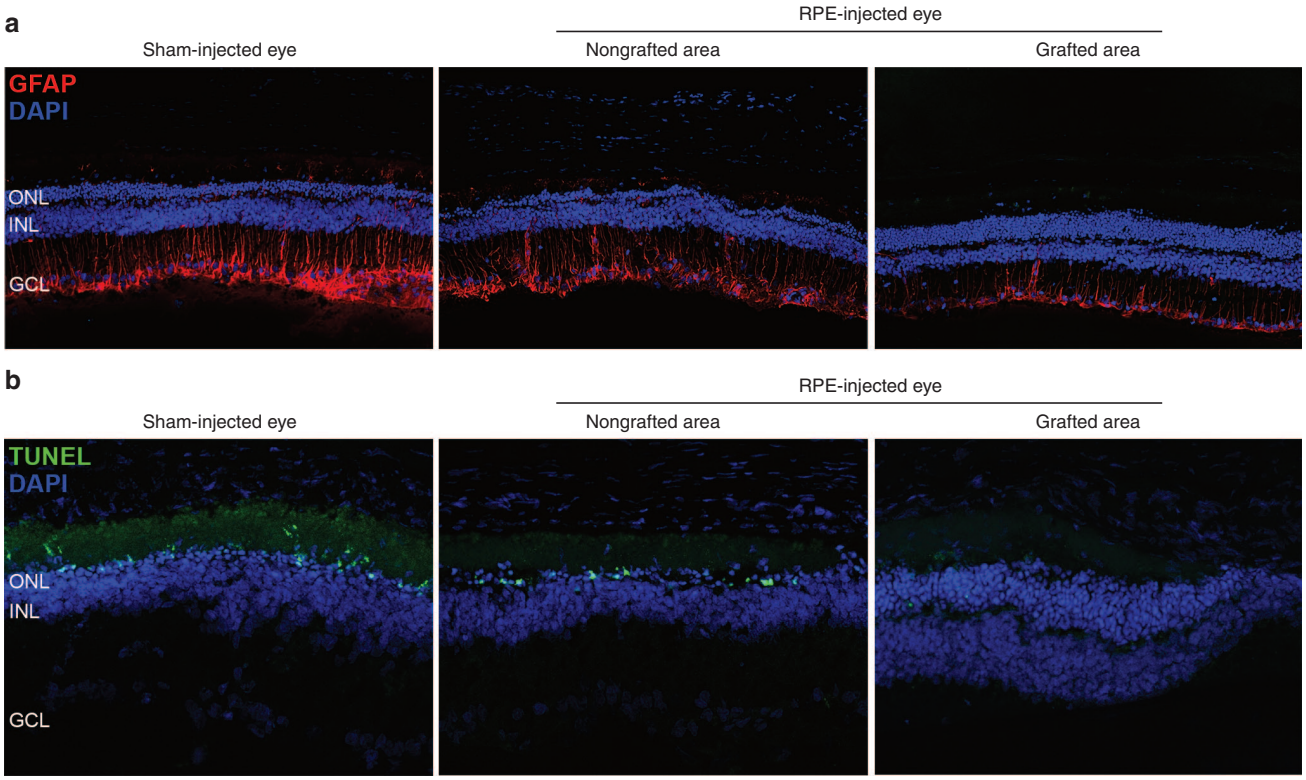

Figure 5 Human cells reduce gliosis and apoptosis of rat retinas. (**a**) Reactive gliosis detected by immunofluorescence with the GFAP antibody was clearly decreased in grafted regions compared with nongrafted regions of the same eye and with sham-injected eyes. (**b**) TUNEL analysis showed a clear reduction in the number of photoreceptor apoptotic nuclei in grafted regions of RPE-injected eyes. Note that all pictures were obtained using the same beam intensity. ONL, outer nuclear layer; INL, inner nuclear layer; GCL, ganglion cell layer.

at 12 weeks PI human cells were still grafted. In fact, recent work has shown that a second transplantation cannot prolong the therapeutic effect.[34] Third, RPE could be combined with photoreceptor transplantation, to replace damaged cells as well as to provide support to both transplanted and still healthy host photoreceptors. However, it is worth noting that the RCS rat model displays a more severe phenotype and faster retinal degeneration than humans affected by RP disease, which typically lose night vision in adolescence, side vision in young adulthood, and central vision later in life.[3] Therefore, the "RPE-alone" cell therapy may prevent photoreceptor cells from degeneration during longer periods in humans than in rats.

To determine the feasibility of cell replacement therapy as a generic treatment for retinal disease, transplantation must be assessed at different stages of retinal degeneration to define the potential breadth of application and to outline therapeutic time windows.[35] For this reason, we tested the effect of RPE cell therapy at two different disease stages: P21 and P42. Previous work had found that grafts were totally ineffective at the latter time point,[20] but here, as also found by Wang *et al.*[36] grafting ARPE-19 cells, we showed that the human RPE-derived cells transplanted at P42 were able to preserve the retina from degeneration in terms of ONL cell rows. However, ERGs responses were null in grafted, nongrafted areas, and in sham-injected eyes when transplanted at P42, highlighting the need to perform transplantation at early stages of the disease to effectively rescue the photoreceptors cells.

The increased visual response and preservation of ONL observed in grafted areas could be due to a direct effect of human RPE cells on photoreceptor debris phagocytosis and visual cycle, or to a paracrine neuroprotective effect. Our *in vitro* expression assays of differentiated RPE cells showed increased expression of *PEDF*, a neurotrophic growth factor known to exert protective effects on retinal neurons.[37,38] These data, together with the fact that the area of preservation extended beyond the defined region covered by the graft, suggest that PEDF or other "diffusible neuroprotective factors" might be partially responsible for the rescue of the phenotype. In this regard, several studies based on intravitreous injections of PSC-derived RPE cells or subretinal transplantation of fibroblasts or feeder cells have shown that at least some cell-specific features are required for the beneficial effects of the treatment.[12,34,39]

Over the last decades, gene therapy has shown a great potential to treat diseases with a genetic component, inherited RD among them. However, the use of this technique requires identification of the molecular cause in each patient and this is particularly complicated in RP cases owing to the genetic complexity of the disease. Moreover, gene therapy is not suitable for approximately the 40% of RP cases that currently remain genetically unsolved.[40] Taken together, these obstacles highlight the need of a "universal" therapeutic approach that uniformly treats all different forms of RP. Within this context, stem cell-based treatments might be an excellent therapeutic strategy, since it is appropriate not only for the genetically diagnosed RP cases, but also for those patients affected by orphaned or novel genes, or by genetically complex RD, such as age-related macular degeneration and diabetic retinopathy.

To the best of our knowledge, this is the first report comparing the therapeutic effects of human RPE cells differentiated from human embryonic stem cells and human-induced pluripotent stem cells. Our data clearly show that RPE derived from either PSC source are equally effective in protecting the retina of RCS rats from degeneration. However, several aspects other than effectiveness must be taken into account when choosing the appropriate cell-based therapy for RPE

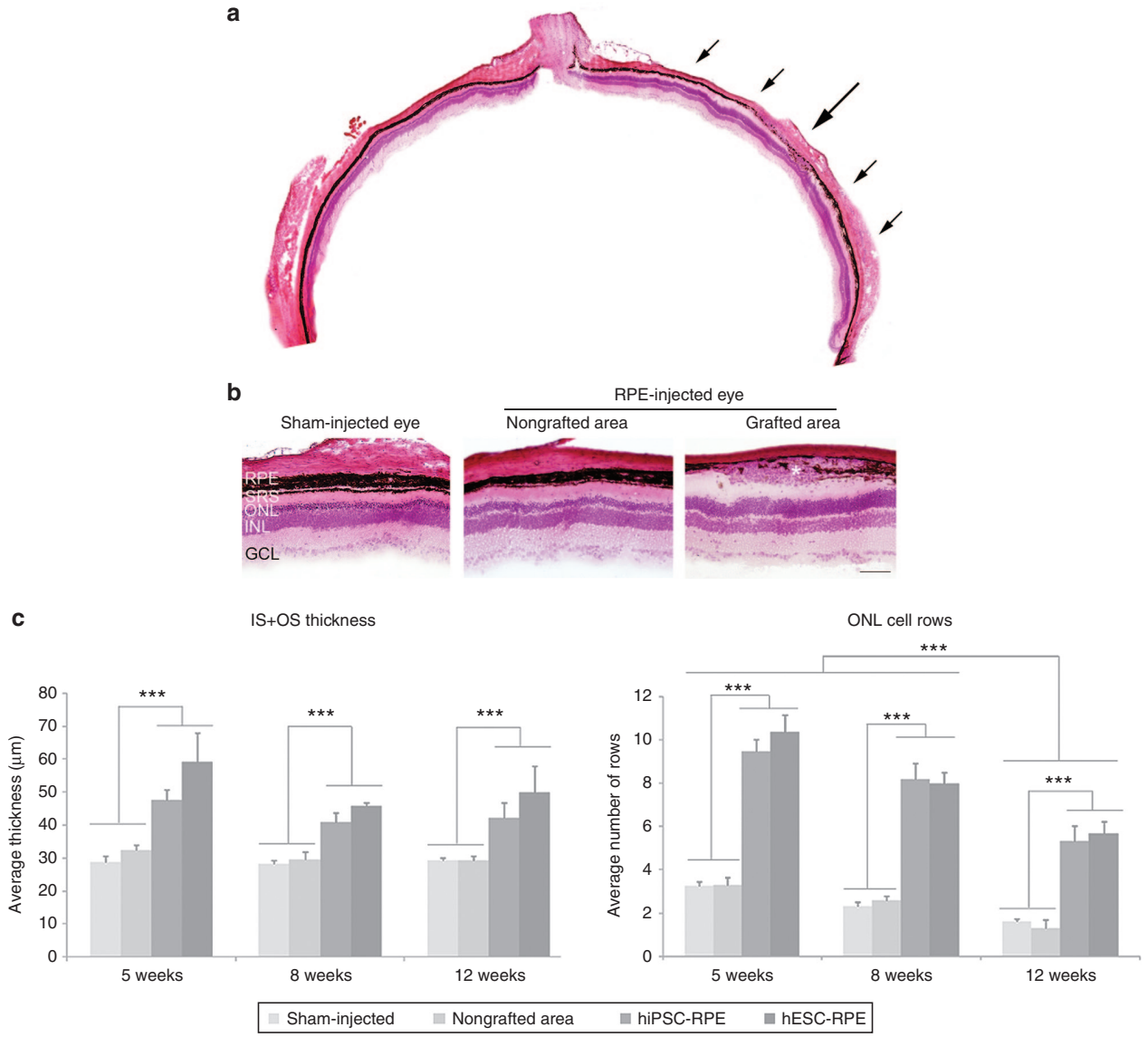

Figure 6 Photoreceptor cell layers are preserved in grafted areas. (**a**) Images of H&E-stained sections showing preservation of layers in proximity to a subretinal RPE graft (located between arrows) compared with thin layers distant from the graft. (**b**) Higher magnifications clearly showed retinal cell layer preservation in proximity to grafted cells (asterisk). (**c**) IS+OS thickness as well as the number of ONL cell rows were significantly increased in grafted areas compared with nongrafted areas and sham-injected eyes up to 12 weeks PI. There was no statistically significant difference between eyes injected with hiPSC ($n = 8$) or hESC ($n = 5$) for IS+OS thickness or number of ONL cell rows. Bar: **b**, 100 µm. Data are presented as mean ± SEM, ***$P < 0.0001$. RPE, retinal pigment epithelium; SRS, subretinal space; ONL, outer nuclear layer; INL, inner nuclear layer; GCL, ganglion cell layer, IS, inner segment, OS, outer segment.

regeneration in humans, including safety issues and considerations of reproducibility, scalability, and affordability, and as well as being ethically acceptable.[41] At any rate, building on the positive results obtained here from the transplantation of the two cell lines, more experiments are warranted with a higher number of samples, to be able to confirm that iPSCs derived from different cell lines and different cell types are suitable for differentiation into RPE, and whether all of them behave as observed in this work.

MATERIAL AND METHODS

Cell culture and differentiation

Two human pluripotent stem cell lines (hPSC), one hiPSC (CBiPSC30-4F-5) and one hESC (ES[4]), were differentiated into RPE cells following the Idelson *et al*. protocol[12], with minor modifications (see Supplementary Materials and Methods and Supplementary Figure S1).

Immunocytochemistry of differentiated cells

Once differentiated, the hPSC-derived RPE cells were characterized by immunocytochemistry to determine the extent of expression of the retinal and RPE differentiation markers. Cells were grown in polystyrene slide-flasks and fixed with 4% (w/v) paraformaldehyde for 20 minutes at room temperature (RT). The immunodetection was performed with TBS/0.2% (v/v) Triton X-100 for permeabilization, and samples were blocked using a solution containing 3% (v/v) goat serum, 1% (v/v) BSA, and 0.3% (v/v) Triton X-100 in PBS for 1 hour at RT. Primary antibodies were incubated at 4 °C overnight, and secondary antibodies were

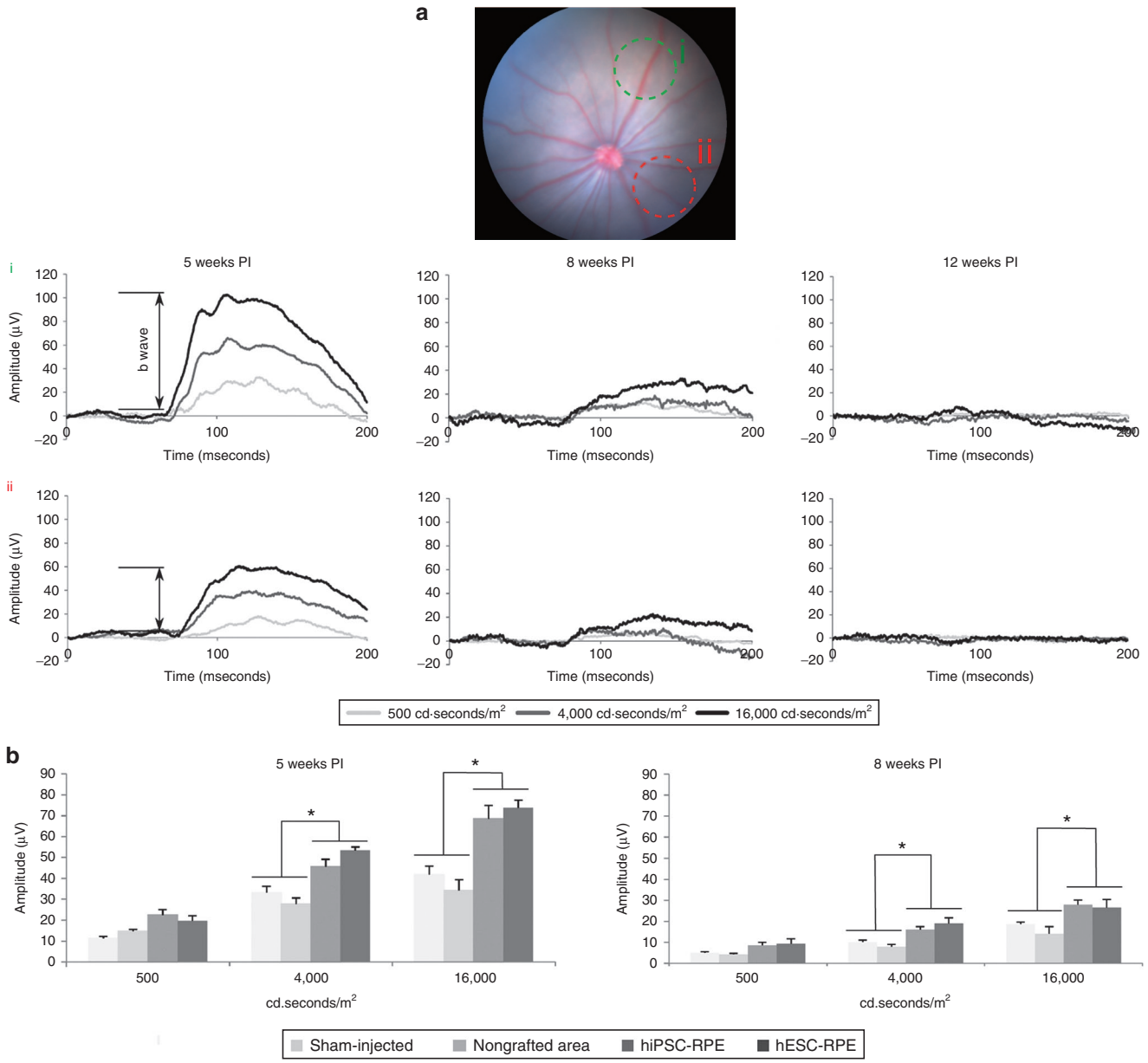

Figure 7 Visual function is conserved in grafted areas. (**a**) Fundus image of an RPE-injected RCS rat and its ERG responses are shown as a representative example. Focal ERG was used to test the functional rescue of transplanted RPE cells at 5, 8, and 12 weeks PI. For each transplanted eye, three different light intensities (500, 4,000 and 16,000 cd seconds/m^2) were used to measure the electrical activity, which was recorded over two different spots in each eye: one over the grafted area (green circle, i) and other over a region far away from the graft, nongrafted area (red circle, ii). (**b**) Grafted areas showed significantly higher b-wave amplitudes than nongrafted and sham-injected eyes when stimulated with 4,000 or 16,000 cd·seconds/m^2. Higher b-wave amplitudes were obtained in grafted regions after 5 ($n = 9$) and 8 ($n = 7$) weeks PI, while no difference was detected after 12 weeks. At 8 weeks, PI b-wave amplitudes were clearly attenuated, but preservation of visual function was still observed. No difference could be detected between hESC- or hiPSC-injected eyes. Data are presented as mean ± SEM, *$P < 0.01$.

incubated at 37 °C for 2 hours. The antibodies used are listed in the Supplementary Table S1. Undifferentiated hPSC were used as negative controls. Samples were mounted in Fluoroshield with DAPI, and images were obtained on an SPE confocal microscopy (Leica Microsystems, Wetzlar, Germany).

Determination of RNA expression by quantitative real-time PCR

Samples from hPSC-derived RPE were taken from each cell line differentiation culture. Cells were treated with Trizol reagent and RNA was isolated using RNeasy RNA isolation kit (Qiagen, Hilden, Germany) following the manufacturer's instructions. RNA was quantified using NanoDrop, and cDNA was synthesized from 1 µg total RNA per sample using the Cloned AMV First-Strand Synthesis Kit (Invitrogen, Life Technologies, Carlsbad, CA). Quantitative real-time PCR (qRT-PCR) was performed with Platinum SYBR Green quantitative PCR super mix (Invitrogen, Life Technologies) with 25 ng cDNA per well. Relative gene expression was assayed in triplicate, and compared with the undifferentiated hPSC cell sample, which served as the zero set point. All qRT-PCR reactions were performed in an Applied Biosystem 7900 HT Fast qRT-PCR System Thermocycler following the manufacturer's instructions. The markers used for the analysis of gene expression were *CRALBP*, *DKK-1*, *MERKT*, *MITF*,

OCT3/4, *OTX2*, *PAX6*, *PEDF*, *RHH*, *RX*, *SIL*, and *TYR*. *GAPDH* was used for normalization. Primer sequences are given in Supplementary Table S2.

Transplantation of differentiated cells into the RCS rat

Before surgery, cells were harvested and transiently labelled with 20 µmol/l Cell Tracker Green CMFDA (Life Technologies, Cat. No. C2925) for 30 minutes at 37 °C, and then washed and suspended in the RPE differentiation medium at a density of 5×10^4 cells/µl. Roughly 100,000 cells in suspension were transplanted into the subretinal space of RCS rats as previously described by Warfvinge *et al*.,[42] but with minor modifications (see Supplementary Materials and Methods and Supplementary Video S1).

We initially injected 123 eyes, 95 of them with RPE-differentiated cells, and 28 with differentiation medium (Table 1). Following transplantation, the fundi of the rats were visualized in a Micron III platform (Phoenix Research Laboratories, Pleasanton, CA), and green fluorescence was used to determine both the injection site and the subretinal area covered by the transplanted cells at the time of injection. We excluded those eyes that did not present an observable fluorescent bleb of cells in the subretinal space, the cases in which injected cells were found in the vitreous and, eyes where major hemorrhage was caused by the intervention ($n = 15$). Thus, we included in the final study 108 eyes: 82 RPE-injected eyes (39 injected with hESC-derived RPE cells and 43 with hiPSC-derived RPE) and 26 sham-injected eyes. To assess the efficacy of the treatment in distinct phases of retinal degeneration, animals were injected either at P21, when the first morphological changes can be noticed in the retina, or at a later stage of the disease, P42, when apoptosis has already caused the death of a significant number of photoreceptor cells.[43,44] RPE- and sham-injected eyes were monitored at 5, 8 or 12 weeks PI. Accordingly, animals were divided into groups on the basis of the type of injected material (hESC-, hiPSC-derived RPE cells, or medium), the postnatal day of injection (P21 or P42), and the end of the experiment (5, 8 or 12 weeks PI) (Table 1).

Immunosuppression by cyclosporin A

To prevent transplant rejection, animals were immune suppressed by the addition of 21 mg/kg/day of cyclosporin A (CsA) (Novartis, Cat. No. 653833.3) to 1 ml of sucralose (Clear H_2O, Cat. No. 74-02-5022), starting the treatment 2 days before the injection and maintaining it throughout the whole experiment. Every 2–3 weeks from the beginning of the treatment, a complete blood count (CBC) (BC-2800Vet, Minidray) on 20 µl of peripheral blood provided the state of immune suppression of the animals. Independently from the period of treatment, all animals were successfully immune suppressed, showing white blood cell levels below the reference range, with no major alterations in the other hematological parameters (see Supplementary Figure S5).

Histology

Fourteen-micrometer cryosections on polylysine-covered slides were fixed with a mixture of methanol and acetic acid (95:5 v:v) for 1 minute at −20°C and stained with hematoxylin/eosin by standard protocols to assess the injection site, retinal lamination and any evidence of tumor formation. ImageJ software was used to measure the number of cell rows of the ONL and the thickness of the inner (IS) and OS of RPE- and sham-injected eyes. For the RPE-injected eyes, two measurements were taken in the same eye: one over the grafted area and another over the nongrafted area, distant from the injection site. For statistical analyses, the significance was calculated with ANOVA, followed by the Tukey test.

Immunohistochemistry

Eyes were excised, frozen in OCT (Tissue-Tek, Sakura Finetech, Torrance, CA) and sectioned for histological and immunohistochemical analyses, or the RPE was removed intact as a flat-mount preparation.

Immunostaining of cryosections. Slides were dried for 1 hour at RT, fixed with paraformaldehyde 4% (w/v) (Electron Microscopy Sciences Cat. No. 15710, Hatfield, PA) for 20 minutes at 37 °C, and washed with PBS. Samples were blocked for 1 hour at RT with a solution containing 3% (v/v) sheep serum, 1% (v/v) BSA and 0.3% (v/v) Triton X-100 in PBS and incubated over night at 4 °C with the primary antibody of interest. Sections were rinsed with PBS and incubated for 1 hour at RT with the corresponding secondary antibody. Sections were mounted in Fluoroshield with DAPI (Sigma-Aldrich, Cat. No. F6057, St. Louis, MO) and analyzed by confocal microscopy (FV1000 Olympus, Center Valley, PA). Details of the antibodies and dilutions used for immunofluorescence, including the human-specific marker antibody cocktail (HSM), are listed in Supplementary Table S1.

Immunostaining of flat-mount preparations. Eyes were enucleated with the aid of a dissecting microscope. The anterior segment and lens were removed, and the retinas were detached, separated from the optic nerve head with fine-curved scissors, and discarded. Radial cuts were made towards the optic nerve head, and the sclera–choroid–RPE complexes (eyecups) were fixed in 100% methanol for 30 minutes at −20 °C. After fixation, eyecups were washed with PBS containing 0.1% (v/v) Triton X-100, blocked with PBS containing 0.1% (v/v) Triton X-100 and 1% (v/v) BSA for 1 hour at RT and incubated overnight at 4 °C with the primary antibodies of interest. Thereafter they were washed and incubated with the corresponding secondary antibodies for 1 hour. Posterior segments were washed in PBS, flat mounted in Fluoroshield with DAPI and analyzed by confocal microscopy (FV1000 Olympus). Antibodies and dilutions used for immunofluorescence in flat-mounted eyes are listed in Supplementary Table S1.

Transmission electron microscopy

hPSC-derived RPE homogeneous culture samples were fixed with 2.5% (w/v) glutaraldehyde for 2 hours at 4 °C. Postfixation was carried out in 1% (w/v) osmium tetroxide for 2 hours at 4 °C, and samples were then dehydrated with ethanol and embedded in epoxy resin. Semithin and ultrathin sections were analyzed. Samples were examined in a Jeol 1011 transmission electron microscope (Jeol, Tokyo, Japan).

Ocular samples containing retina, RPE, choroid, and sclera were dissected out of from RPE- and sham-injected eyes. In addition, comparable samples from noninjected Long–Evans wild-type rats were obtained. Samples were fixed in 2.5% (v/v) glutaraldehyde and 2% (w/v) paraformaldehyde and postfixed in 1% (w/v) osmium tetroxide. After staining in aqueous uranyl acetate, samples were dehydrated and embedded in epoxy resin. Semithin sections stained with methylene blue were examined by light microscopy and ultrathin sections (70 nm) stained with uranyl acetate and lead citrate were examined in a Jeol 1400 transmission electron microscope (Jeol).

TUNEL analyses

Fourteen-micrometer cryosections on polylysine-covered slides were fixed with paraformaldehyde 4% (v/v) for 20 minutes at 37 °C, washed with PBS, and permeabilized with proteinase K (20 µg/ml) for 15 minutes at RT. The TUNEL reaction was performed using the Click-iT Plus TUNEL Assay (Life technologies, Cat. No. C10617) following the manufacturer's instructions. A positive control section was obtained by inducing DNA strand breaks with 1 unit of DNAse I. A negative control section was treated with a TUNEL cocktail lacking the TdT enzyme. Sections were mounted in Fluoroshield with DAPI (Sigma-Aldrich, Cat. No. F6057) and analyzed by confocal microscopy (FV1000 Olympus).

Focal ERG

To assess transplantation efficiency, retinas were examined at 5, 8, and 12 weeks PI by live imaging and focal ERG, which allows the measurement of the visual response limited to particular areas. Recordings were measured using the Micron III platform (Phoenix Research Laboratories). Dark-adapted rats (12–16 hours) were anaesthetized under dim red light with 2% (v/v) isoflurane gas and placed on a heating pad at 37 °C. Pupils were dilated with a topical mixture of phenylephrine and tropicamide, and recordings were measured as previously described.[30] A spot of ~2 mm diameter on the retina was stimulated at different light intensities (500, 4,000, and 16,000 cd·seconds/m^2) over two distinct regions of RPE-injected eyes, the grafted area and the nongrafted area, and over the injected area of sham-injected eyes. At least five ERG traces were obtained for each condition and results averaged. The amplitude and the implicit time of the b-wave were calculated using the Labscribe2 software. For statistical analyses, the significance was calculated with ANOVA followed by Tukey test.

All procedures on RCS rats were carried out with the approval of the Ethics Committee for Animal Experimentation of the Hospital Universitari Vall d'Hebron, and in accordance with the ARVO Statement for the Use of Animals in Ophthalmic and Vision Research and with the Declaration of Helsinki.

CONFLICT OF INTERESTS

The authors declare no conflicts of interest.

ACKNOWLEDGMENTS

The authors thank Verónica Melgarejo, Ángel Vázquez, Cristina Gómez Santos, Lola Mulero Pérez, Cristina Morera Albert and Mercè Marti Gaudes (CMRB Core Facility) for technical assistance, and Trevor G. Cooper for language editing. This research project was funded by grants from *La Marató de TV3* (project no. 484/C/2012) and by the post-doc fellowship (SFRH/BPD/102573/2014) from the Fundação para a Ciência e a Tecnologia, Ministério da Educação e Ciência, Portugal.

REFERENCES

1. Strauss, O (2005). The retinal pigment epithelium in visual function. *Physiol Rev* **85**: 845–881.
2. Ramsden, CM, Powner, MB, Carr, AJ, Smart, MJ, da Cruz, L and Coffey, PJ (2013). Stem cells in retinal regeneration: past, present and future. *Development* **140**: 2576–2585.
3. Hartong, DT, Berson, EL and Dryja, TP (2006). Retinitis pigmentosa. *Lancet* **368**: 1795–1809.
4. Churchill, JD, Bowne, SJ, Sullivan, LS, Lewis, RA, Wheaton, DK, Birch, DG *et al.* (2013). Mutations in the X-linked retinitis pigmentosa genes RPGR and RP2 found in 8.5% of families with a provisional diagnosis of autosomal dominant retinitis pigmentosa. *Invest Ophthalmol Vis Sci* **54**: 1411–1416.
5. Zheng, A, Li, Y and Tsang, SH (2015). Personalized therapeutic strategies for patients with retinitis pigmentosa. *Expert Opin Biol Ther* **15**: 391–402.
6. Musarella, MA and Macdonald, IM (2011). Current concepts in the treatment of retinitis pigmentosa. *J Ophthalmol* **2011**: 753547.
7. Lamba, DA, McUsic, A, Hirata, RK, Wang, PR, Russell, D and Reh, TA (2010). Generation, purification and transplantation of photoreceptors derived from human induced pluripotent stem cells. *PLoS One* **5**: e8763.
8. Wiley, LA, Burnight, ER, Songstad, AE, Drack, AV, Mullins, RF, Stone, EM *et al.* (2015). Patient-specific induced pluripotent stem cells (iPSCs) for the study and treatment of retinal degenerative diseases. *Prog Retin Eye Res* **44**: 15–35.
9. Borooah, S, Phillips, MJ, Bilican, B, Wright, AF, Wilmut, I, Chandran, S *et al.* (2013). Using human induced pluripotent stem cells to treat retinal disease. *Prog Retin Eye Res* **37**: 163–181.
10. Rowland, TJ, Blaschke, AJ, Buchholz, DE, Hikita, ST, Johnson, LV and Clegg, DO (2013). Differentiation of human pluripotent stem cells to retinal pigmented epithelium in defined conditions using purified extracellular matrix proteins. *J Tissue Eng Regen Med* **7**: 642–653.
11. Lamba, DA, Karl, MO, Ware, CB and Reh, TA (2006). Efficient generation of retinal progenitor cells from human embryonic stem cells. *Proc Natl Acad Sci USA* **103**: 12769–12774.
12. Idelson, M, Alper, R, Obolensky, A, Ben-Shushan, E, Hemo, I, Yachimovich-Cohen, N *et al.* (2009). Directed differentiation of human embryonic stem cells into functional retinal pigment epithelium cells. *Cell Stem Cell* **5**: 396–408.
13. Mekala, SR, Vauhini, V, Nagarajan, U, Maddileti, S, Gaddipati, S and Mariappan, I (2013). Derivation, characterization and retinal differentiation of induced pluripotent stem cells. *J Biosci* **38**: 123–134.
14. Hansson, ML, Albert, S, González Somermeyer, L, Peco, R, Mejía-Ramírez, E, Montserrat, N *et al.* (2015). Efficient delivery and functional expression of transfected modified mRNA in human embryonic stem cell-derived retinal pigmented epithelial cells. *J Biol Chem* **290**: 5661–5672.
15. Wong, GK and Chiu, AT (2011). Gene therapy, gene targeting and induced pluripotent stem cells: applications in monogenic disease treatment. *Biotechnol Adv* **29**: 1–10.
16. Pinilla, I, Cuenca, N, Sauvé, Y, Wang, S and Lund, RD (2007). Preservation of outer retina and its synaptic connectivity following subretinal injections of human RPE cells in the Royal College of Surgeons rat. *Exp Eye Res* **85**: 381–392.
17. Bourne, MC, Campbell, DA and Tansley, K (1938). Hereditary degeneration of the rat retina. *Br J Ophthalmol* **22**: 613–623.
18. D'Cruz, PM, Yasumura, D, Weir, J, Matthes, MT, Abderrahim, H, LaVail, MM *et al.* (2000). Mutation of the receptor tyrosine kinase gene Mertk in the retinal dystrophic RCS rat. *Hum Mol Genet* **9**: 645–651.
19. Cuenca, N, Pinilla, I, Sauvé, Y and Lund, R (2005). Early changes in synaptic connectivity following progressive photoreceptor degeneration in RCS rats. *Eur J Neurosci* **22**: 1057–1072.
20. Li, L and Turner, JE (1991). Optimal conditions for long-term photoreceptor cell rescue in RCS rats: the necessity for healthy RPE transplants. *Exp Eye Res* **52**: 669–679.
21. Lund, RD, Adamson, P, Sauvé, Y, Keegan, DJ, Girman, SV, Wang, S *et al.* (2001). Subretinal transplantation of genetically modified human cell lines attenuates loss of visual function in dystrophic rats. *Proc Natl Acad Sci USA* **98**: 9942–9947.
22. Lawrence, JM, Sauvé, Y, Keegan, DJ, Coffey, PJ, Hetherington, L, Girman, S *et al.* (2000). Schwann cell grafting into the retina of the dystrophic RCS rat limits functional deterioration. Royal College of Surgeons. *Invest Ophthalmol Vis Sci* **41**: 518–528.
23. Coffey, PJ, Girman, S, Wang, SM, Hetherington, L, Keegan, DJ, Adamson, P *et al.* (2002). Long-term preservation of cortically dependent visual function in RCS rats by transplantation. *Nat Neurosci* **5**: 53–56.
24. Wang, S, Lu, B, Wood, P and Lund, RD (2005). Grafting of ARPE-19 and Schwann cells to the subretinal space in RCS rats. *Invest Ophthalmol Vis Sci* **46**: 2552–2560.
25. Inoue, Y, Iriyama, A, Ueno, S, Takahashi, H, Kondo, M, Tamaki, Y *et al.* (2007). Subretinal transplantation of bone marrow mesenchymal stem cells delays retinal degeneration in the RCS rat model of retinal degeneration. *Exp Eye Res* **85**: 234–241.
26. Wang, S, Girman, S, Lu, B, Bischoff, N, Holmes, T, Shearer, R *et al.* (2008). Long-term vision rescue by human neural progenitors in a rat model of photoreceptor degeneration. *Invest Ophthalmol Vis Sci* **49**: 3201–3206.
27. Thumann, G, Salz, AK, Walter, P and Johnen, S (2009). Preservation of photoreceptors in dystrophic RCS rats following allo- and xenotransplantation of IPE cells. *Graefes Arch Clin Exp Ophthalmol* **247**: 363–369.
28. Vugler, A, Carr, AJ, Lawrence, J, Chen, LL, Burrell, K, Wright, A *et al.* (2008). Elucidating the phenomenon of HESC-derived RPE: anatomy of cell genesis, expansion and retinal transplantation. *Exp Neurol* **214**: 347–361.
29. Carr, AJ, Vugler, AA, Hikita, ST, Lawrence, JM, Gias, C, Chen, LL *et al.* (2009). Protective effects of human iPS-derived retinal pigment epithelium cell transplantation in the retinal dystrophic rat. *PLoS One* **4**: e8152.
30. Krohne, TU, Westenskow, PD, Kurihara, T, Friedlander, DF, Lehmann, M, Dorsey, AL *et al.* (2012). Generation of retinal pigment epithelial cells from small molecules and OCT4 reprogrammed human induced pluripotent stem cells. *Stem Cells Transl Med* **1**: 96–109.

31. Georgiadis, A, Tschernutter, M, Bainbridge, JW, Balaggan, KS, Mowat, F, West, EL *et al.* (2010). The tight junction associated signalling proteins ZO-1 and ZONAB regulate retinal pigment epithelium homeostasis in mice. *PLoS One* **5**: e15730.
32. Kennedy, CJ, Rakoczy, PE and Constable, IJ (1995). Lipofuscin of the retinal pigment epithelium: a review. *Eye (Lond)* **9**: 763–771.
33. Wu, KH, Madigan, MC, Billson, FA and Penfold, PL (2003). Differential expression of GFAP in early v late AMD: a quantitative analysis. *Br J Ophthalmol* **87**: 1159–1166.
34. Tzameret, A, Sher, I, Belkin, M, Treves, AJ, Meir, A, Nagler, A *et al.* (2014). Transplantation of human bone marrow mesenchymal stem cells as a thin subretinal layer ameliorates retinal degeneration in a rat model of retinal dystrophy. *Exp Eye Res* **118**: 135–144.
35. Barber, AC, Hippert, C, Duran, Y, West, EL, Bainbridge, JW, Warre-Cornish, K *et al.* (2013). Repair of the degenerate retina by photoreceptor transplantation. *Proc Natl Acad Sci USA* **110**: 354–359.
36. Wang, S, Lu, B, Girman, S, Holmes, T, Bischoff, N and Lund, RD (2008). Morphological and functional rescue in RCS rats after RPE cell line transplantation at a later stage of degeneration. *Invest Ophthalmol Vis Sci* **49**: 416–421.
37. Cao, W, Tombran-Tink, J, Elias, R, Sezate, S, Mrazek, D and McGinnis, JF (2001). *In vivo* protection of photoreceptors from light damage by pigment epithelium-derived factor. *Invest Ophthalmol Vis Sci* **42**: 1646–1652.
38. Pang, IH, Zeng, H, Fleenor, DL and Clark, AF (2007). Pigment epithelium-derived factor protects retinal ganglion cells. *BMC Neurosci* **8**: 11.
39. Wang, NK, Tosi, J, Kasanuki, JM, Chou, CL, Kong, J, Parmalee, N *et al.* (2010). Transplantation of reprogrammed embryonic stem cells improves visual function in a mouse model for retinitis pigmentosa. *Transplantation* **89**: 911–919.
40. Wang, F, Wang, Y, Zhang, B, Zhao, L, Lyubasyuk, V, Wang, K *et al.* (2014). A missense mutation in HK1 leads to autosomal dominant retinitis pigmentosa. *Invest Ophthalmol Vis Sci* **55**: 7159–7164.
41. Mount, NM, Ward, SJ, Kefalas, P and Hyllner, J (2015). Cell-based therapy technology classifications and translational challenges. *Philos Trans R Soc Lond B Biol Sci* **370**: 20150017.
42. Warfvinge, K, Kamme, C, Englund, U and Wictorin, K (2001). Retinal integration of grafts of brain-derived precursor cell lines implanted subretinally into adult, normal rats. *Exp Neurol* **169**: 1–12.
43. Davidorf, FH, Mendlovic, DB, Bowyer, DW, Gresak, PM, Foreman, BC, Werling, KT *et al.* (1991). Pathogenesis of retinal dystrophy in the Royal College of Surgeons rat. *Ann Ophthalmol* **23**: 87–94.
44. Tso, MO, Zhang, C, Abler, AS, Chang, CJ, Wong, F, Chang, GQ *et al.* (1994). Apoptosis leads to photoreceptor degeneration in inherited retinal dystrophy of RCS rats. *Invest Ophthalmol Vis Sci* **35**: 2693–2699.

Supplementary Information accompanies this paper on the *Molecular Therapy—Methods & Clinical Development* website (http://www.nature.com/mtm)